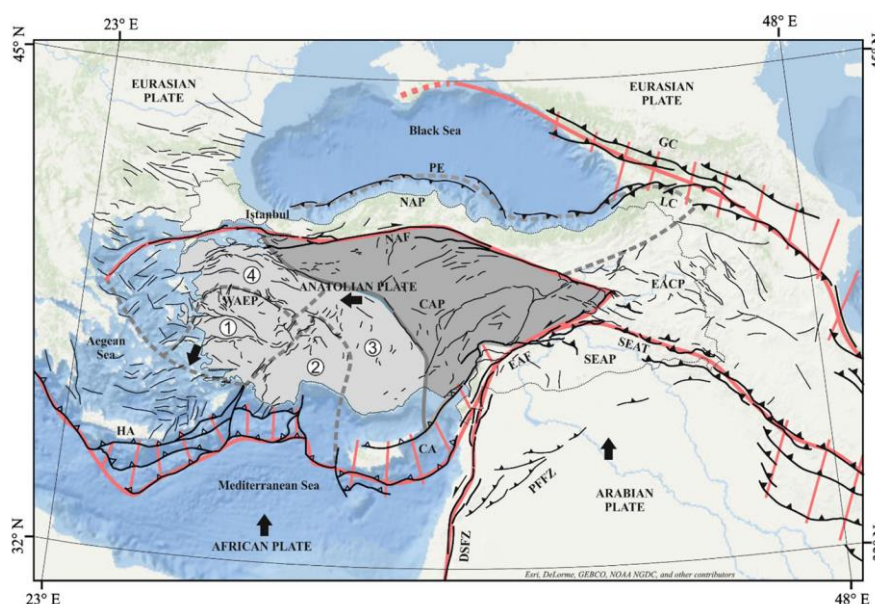




32 NAF(North Anatolian Fault) is a tectonic plate boundary between Anatolian and Eurasian
33 plates. It slowly moves ~20 mm/year to the west by the overthrusting Arabian plate from the south
34 and compresses the plate motion with the help of a massive Eurasian plate in the north. These tectonic
35 forces constitute North Anatolian Fault, which lies between Karliova triple junction from the east to
36 the Aegean Sea to the west for almost 1200 km long. It extends from 100 m to 10 km along the zone
37 and south part, Anatolian plate, moves 20-25 mm/year to the west relative to the Eurasian plate. The
38 velocity changes along the fault, west region moves faster than the eastern part, and is a right-lateral
39 strike slip fault (Fig. 1)(Ketin 1969-1976, McClusky et al. 2000, Cakir et al. 2005, Şengör et al. 2005,
40 Reilinger et al. 2006, Yavaşoğlu et al. 2011, Bohnhoff et al. 2016).

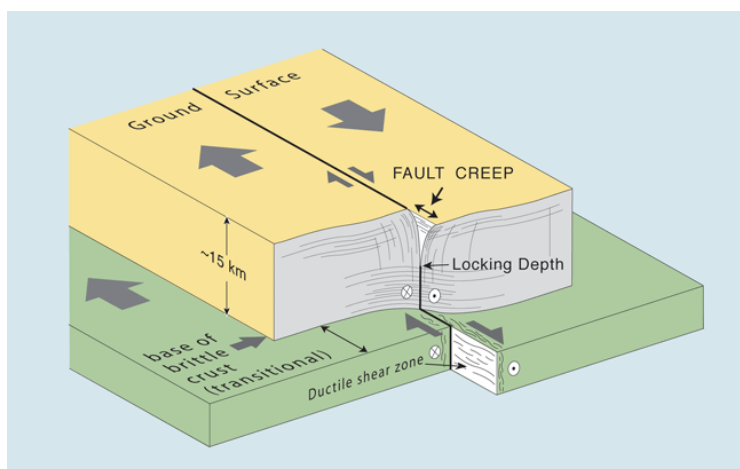


41
42 **Figure 1.** Formation of the North Anatolian Fault and interacting tectonic plates (from Emre et al.
43 2018). Anatolian plate moves westwards due to African and Arabian plates overthrusting. (1) West
44 Anatolian graben systems, (2) Outer Isparta Angle, (3) Inner Isparta Angle, and (4) Northwest
45 Anatolia transition zone. The original version of the figure is available in Emre et al. 2018.

46 Earthquake mechanism might have different characteristics in some regions. Faults may move
47 freely without an earthquake and this motion reported at some unique places like Hayward fault
48 (Schmidt et al. 2005), the Superstition Hills fault(Wei et al. 2011) and Ismetpasa segments (Cakir et al.
49 2012), and can be observed from the surface(Ambraseys 1970, Yavasoglu et al. 2015). This
50 phenomenon is called “aseismic creep” and may occur in two different ways: If the creep takes place
51 to the bottom of seismogenic layer and the surface velocities are equal or close to the long-term
52 tectonic velocities, there will not be enough strain accumulation for a large scale earthquake (Şaroğlu
53 ve Barka 1995, Cakir et al. 2005). On the other hand, if this free motion is not observed to the bottom



54 of the seismogenic layer or observed surface velocities are smaller than the tectonic velocities, strain
55 will accumulate to a final earthquake (Fig. 2) (Karabacak et al. 2011, Ozener et al. 2013, Yavasoglu et
56 al. 2015). Also, aseismic creep in a region may occur continuously or fade out after some period
57 (Kutoglu et al. 2010).



58

59 **Figure 2.** Aseismic creep structure in a fault zone. Fault may slip freely to some depths and locked
60 after to the bottom (URL-1).

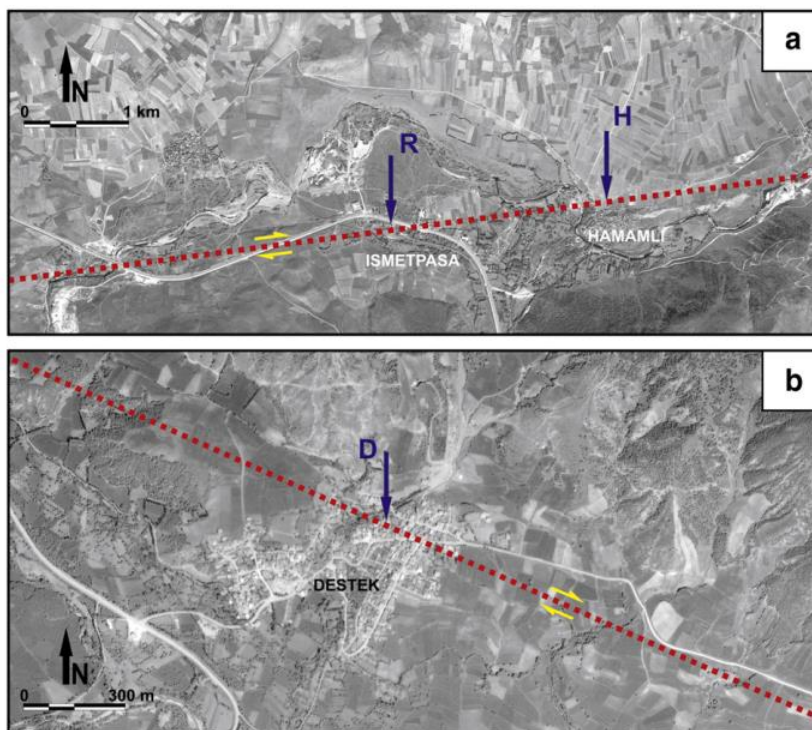
61 NAF reported to have segments which shows aseismic creep until 1970: Ismetpasa and Destek,
62 where the second site is a more recent discovery (Ambraseys 1970, Karabacak et al. 2011). Aseismic
63 creep at the Ismetpasa reported to occur along ~70-80 km from Bayramoren at the east to the Gerece
64 at the west. It was discovered at the wall of the Ismetpasa train station at 1970 and several minor and
65 large scale studies monitored the area until then (Table 1). This segment hosts three destructive
66 earthquakes (1943 Tosya $M_w=7.2$, 1944 Gerece $M_w=7.2$, 1951 Kursunlu $M_w=6.9$) that may have
67 triggered or affect the creep (Şaroğlu ve Barka 1995, Cakir et al. 2005, Karabacak et al. 2011, Kaneko
68 et al. 2013).

69 On the other side, creep at the Destek segment reported at 2003 on a field trip around the
70 region. Unlike the Ismetpasa segment, number of researches at this segment is just a few, and also the
71 length of this segment is unclear, but 1943 Tosya earthquake affected this area (Karabacak et al. 2011)
72 (Table 2).

73 All the studies around these segments indicates the continuity of creep but the results are
74 inconsistent and cannot clearly refer whether this event has an increasing trend or not. Most of the
75 researches (Ambraseys 1970, Aytun 1982, Eren 1984, Altay&Sav 1991, Deniz et al. 1993, Kutoglu et al.
76 2008&2009&2013, Karabacak et al. 2011, Ozener et al. 2013, Bilham et al. 2016) generally are on a
77 micro-scale and focused on the Ismetpasa or a network near this village with geodetic methods, while



78 others on a macro-scale with InSAR (Deguchi 2011, Fialko et al. 2011, Köksal 2011, Kaneko et al. 2013,
79 Cetin et al. 2014, Kutoglu et al. 2013) which needs a ground truth (Fig 3).



80
81 **Figure 3.** Reported aseismic creep zones at Ismetpasa (a) and Destek (b) segments from a recent
82 study. (a) “R” shows creep observed at the wall at the Ismetpasa train station, and “H” shows the
83 creep at Hamamli village. (b) “D” represents the reported creep at Destek town (from Karabacak et
84 al. 2011).

85 These results cannot reveal the creep trend clearly. In addition, a ground network is required
86 to exhibit the fault characteristics clearly along these segments. For this reason, we established a
87 ground network forming profiles around these segments and made three observations annually from
88 2014 to 2016.



89 **Table 1.** Studies and their results to observe aseismic creep at the Ismetpasa segment between 1970-
 90 2016.

Study	Creep rate(cm/year)	Years covered	Method
Ambraseys(1970)	2.0 ± 0.6	1957-1969	Wall offset measurements
Aytun(1982)	1.10 ± 0.11	1969-1978	Doppler
Eren(1984)	1.00 ± 0.40	1972-1982	Trilateration
Deniz et al.(1993)	0.93 ± 0.07	1982-1992	Trilateration
Cakir et al.(2005)	0.80 ± 0.30	1992-2000	InSAR
Kutoglu&Akcin(2006)	0.78 ± 0.05	1992-2002	GPS
Kutoglu et al.(2008)	1.20 ± 0.11	2002-2007	GPS
Kutoglu et al.(2010)	1.51 ± 0.41	2007-2008	GPS
Karabacak et al.(2011) [1.region]	0.84 ± 0.40	2007-2009	LIDAR
Karabacak et al.(2011) [2. region]	0.96 ± 0.40	2007-2009	LIDAR
Deguchi(2011)	1.4	2007-2011	PALSAR
Fialko et al.(2011)	1.0	2007-2010	PALSAR
Ozener et al.(2013)	0.76 ± 0.10	2005-2011	GPS
Köksal(2011)	1.57 ± 0.20	2007-2010	DInSAR
Görmüş(2011)	1.30 ± 0.39	2008-2010	GPS
Kaneko et al.(2013)	0.9 ± 0.2	2007-2011	InSAR
Cetin et al.(2014)	0.8 ± 0.2	2003-2010	InSAR(PSI)
Altay&Sav(1991)	0.76 ± 0.1	1982-1991	Kripmetre
Kutoglu et al.(2013)	1.3 ± 0.2	2008-2010	GPS
Kutoglu et al.(2013)	1.25 ± 0.2	2007-2010	InSAR
Ambraseys(1970) - Bilham et al.(2016) revision	1.04 ± 0.04	1957-1969	Revaluation of photographs
Aytun(1982)	1.50	1957-1969	Revaluation of photographs
Aytun(1982) – Bilham et al.(2016) revision	1.045 ± 0.035	1957-1969	Revaluation of photographs
Bilham et al.(2016)	0.61 ± 0.02	2014-2016	Creepmeter

91 **Table 2.** Studies and their results to observe aseismic creep at the Destek segment.

Study	Creep rate (cm/year)	Years covered	Method
Karabacak et al.(2011)	0.66 ± 0.40	2007-2009	LIDAR
Fraser et al.(2009)	0.6	2009	Trench study

92 **Network Design Around the Creeping Segments**

93 Designing a monitoring network around tectonic structures always related to the geological
 94 characteristics and fault geometry, which includes the locking and earthquake related motions
 95 (coseismic movements) through the fault. Previous studies indicate that the velocities for the stations
 96 distant from the fault plane can be used to derive long-term plate velocities, while nearby station
 97 velocities are suitable to detect the locking depth of a fault (Taskin et al. 2003, Halicioğlu vd. 2009). In
 98 addition, velocities of the observation stations gradually decrease when their locations approach to
 99 the fault plane. Another factor is the number of the stations and this is related to the fault length and
 100 wideness, but the station locations perpendicular to the fault plane must not exceed the ($\pm 1/\sqrt{3}$) of the



101 locking depth. Also, some researches specify this limit to the double of the depth (Taskin et al. 2003,
102 Kutoglu&Akcin 2006, Kutoğlu vd. 2009, Halicioğlu vd. 2009, Poyraz vd. 2011, Bohnhoff et al. 2016). For
103 this purpose, the following equation is used in general to obtain to proper distances of the observation
104 stations from the fault plane:

$$V(x) = \frac{V_T}{\pi} \arctan\left(\frac{x}{D}\right) \quad (1)$$

105 where:

- 106 - V : Fault parallel velocity
- 107 - V_T : Long term tectonic plate velocity
- 108 - x : Distance to fault plane
- 109 - D : Locking depth of the fault(Halicioğlu vd 2009).

110 Location of the stations may vary according to the geological surface elements, but generally
111 established on the both sides of the fault to form a profile on each block to obtain surface velocities
112 (Yavasoglu et al. 2015).

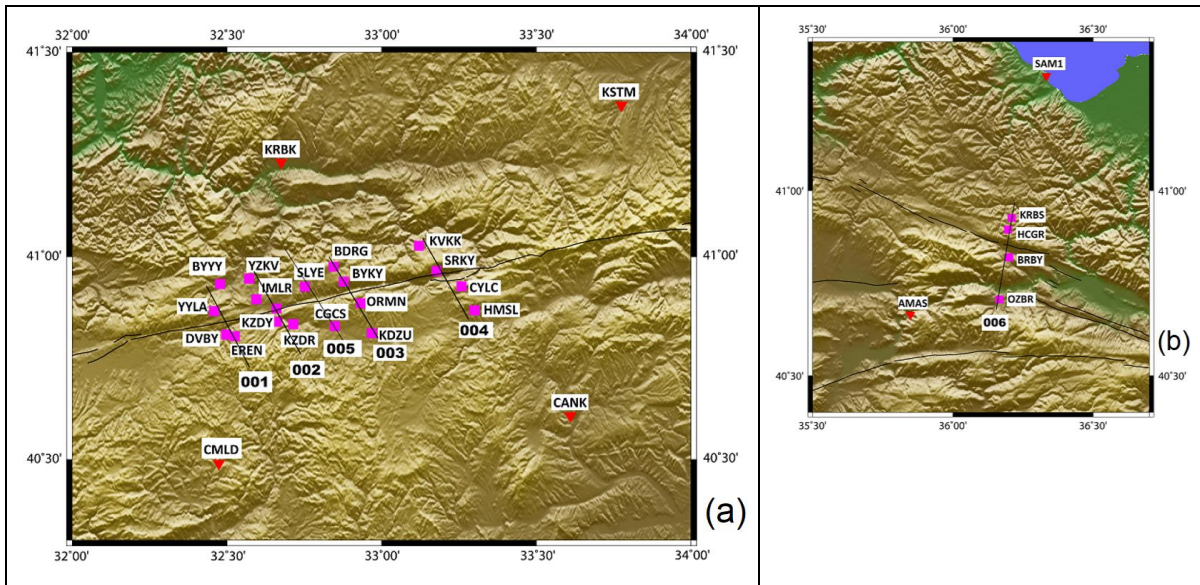
113 Geologic structure at the tectonic block boundaries and fault plane geometry also affects the
114 tectonic behaviour. To better understand this mechanism, established network around the fault zone
115 is observed with different techniques periodically or continuously. The variation of the observations
116 are clues to detect these amplitudes, and GPS is the most common technique for this kind of studies.
117 This technique is very effective and efficient to collect data from ground stations established around
118 the faults (Poyraz vd. 2011, Aladoğan vd. 2017).

119 Profiles intersect with fault plane vertically are used to estimate the locking depth. However,
120 in such regions like Ismetpasa and Destek, there is an additional locking depth deduced from the
121 previous studies, which indicates that the creeping layer of the seismogenic zone does not reach to
122 the bottom, but around 5-7 km depth in these areas (Kaneko et al. 2013, Ozener et al. 2013, Cetin et
123 al. 2014, Bilham et al. 2016, Rousset et al. 2016). For this reason, aseismic layer's attenuation depth is
124 another crucial element to understand the creeping mechanism (Fig 1). Also considering the 5-7 km
125 depth value with the *Eq.1*, station locations are chosen as 3 and 10 km on the both sides of the fault
126 forming profiles, while NAF general locking depth is around 15 km (McClusky et al. 2000, Poyraz vd.
127 2011, Bohnhoff et al. 2016).

128 Before the 3 epochs of observations, a network was planned forming 4 profiles at the
129 Ismetpasa, and 1 profile at the Destek segments and including surrounding continuous GPS
130 stations(Real Time Kinematic Continuously Operating Reference Stations-RTK CORS) (Fig 4). Aim of this
131 study was to monitor this network periodically to calculate the velocity field with combining the results



132 with CORS station velocities and estimate the creep ratio within the Ismetpasa and Destek segments
133 (Yavasoglu et al. 2015).



134 **Figure 4.** Planned profiles and campaign GPS stations(pink) at Ismetpasa(a) on the left and Destek(b)
135 on the right. Profiles 001-004 planned and established on the Ismetpasa segment, and profile 005
136 added to the network using two suitable stations. Profile 006 is on Destek segment. Other
137 continuous GPS sites (RTK CORS) shown in red(after Yavasoglu et al. 2015).

138 While establishing the network, first consideration for 3 and 10 km on the both sides of the
139 fault generally occurred, but some minor changes took place according to the geological structure of
140 the area. In addition, another profile between the 2nd and 3rd profiles formed with the suitable location
141 of two unplanned stations. Finally, there are 5 profiles within ~70 km along the Ismetpasa and 1 profile
142 along the Destek.

143 Observations on the stations completed around the July and August for 3 years using relative
144 geolocation based on carrier phase observations with GPS technique (Table 3). Force centering
145 equipment and GPS masts were used when necessary. First campaign was on the 235-238 and 241 GPS
146 days in 2014, second was on 215-221 GPS days in 2015, and the last one was between 210-220 GPS
147 days in 2016.



148

Table 3. Campaign stations, their locations and facility types.

Profile number	Station ID	Site	Latitude (°)	Longitude (°)	Type of facility
001	BYYY	Büyükayalar	40.49	32.48	Bronze
	YYLA	Yayla Village	41.45	31.78	Bronze
	DVBY	Davutbeyli Village	39.43	32.50	Bronze
	EREN	Elören Village	40.81	32.50	Bronze
002	YZKV	Yazıkavak Village	40.80	32.53	Bronze
	IMLR	İmanlar Village	40.95	32.57	Bronze
	HMMP	Hamamlı Village	40.90	32.60	Pillar
	KZDR	Kuzdere Village	41.23	32.68	Pillar
005 (intermediate)	SLYE	Kapaklı Village	41.85	32.72	Pillar
	CGCS	D100 wayside	39.86	32.85	Pillar
003	BDRG	Boduroğlu Village	39.89	32.76	Bronze
	BYKY	Beyköy Village	40.83	32.85	Pillar
	ORMN	Forest	40.94	32.86	Bronze
	KDZU	Kadıözü Village	40.88	32.93	Pillar
004	KVKK	Kavak Village	40.81	32.97	Bronze
	SRKY	Sarıkaya Village	41.03	33.12	Bronze
	CYLC	Çaylıca Village	40.97	33.18	Bronze
	HMSL	Hacımusla Village	40.93	33.26	Pillar
006	KRBS	Korubaşı Village	40.82	36.20	Bronze
	HCGR	Hacıgeriç Village	40.71	36.17	Bronze
	BRBY	Borabay	40.90	36.20	Pillar
	OZBR	Özbaraklı Village	39.66	35.87	Pillar

149

After the first campaign, KZDY station was damaged and removed from rest of the project. Raw data collected for a minimum of 8 hours at each station for the rest of the project and evaluated with GAMIT/GLOBK software (Herring et al. 2015a, 2015b) at first, then the results used as input to block modelling software TDEFNODE (McCaffrey 2002, 2009). A total of 63 stations (22 campaign, 30 surrounding RTK CORS, 11 IGS) are used in this network to monitor İsmetpaşa and Destek segments and the remaining region between them (Table 4).

155

Table 4. Continuous GPS(RTK CORS) stations and their locations.

Station ID	Province	Station ID	Province	Station ID	Province
AKDG	Yozgat	FASA	Ordu	RDIY	Tokat
AMAS	Amasya	GIRS	Giresun	SAM1	Samsun
ANRK	Ankara	HEND	Sakarya	SIH1	Eskişehir
BILE	Bilecik	HYMN	Ankara	SINP	Sinop
BOLU	Bolu	IZMT	İzmit	SIVS	Sivas
BOYT	Sinop	KKAL	Kırıkkale	SSEH	Sivas
CANK	Çankırı	KRBK	Karabük	SUNL	Çorum
CMLD	Ankara	KSTM	Kastamonu	TOK1	Tokat
CORU	Çorum	KURU	Bartın	VEZI	Samsun
ESKS	Eskişehir	NAHA	Ankara	ZONG	Zonguldak

156



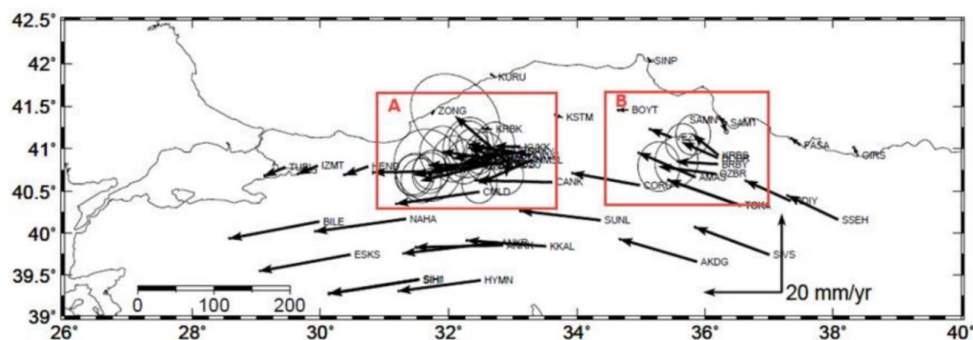
157 **GPS Data Evaluation**

158 In this study, all campaign station observed between 2014-2016 for 3 campaigns and data were
 159 evaluated with GAMIT/GLOBK software. Also, GPS data for cGPS and IGS stations downloaded to cover
 160 every six month between August 2009-2016 to increase the stabilization at the GLOBK step. The
 161 networks linked to the ITRF 2008 global coordinate system by using surrounding IGS sites (Table 5)
 162 (Yavaşoglu et al. 2011, Herring et al. 2015a, 2015b). After the transformation with GLOBK, the root
 163 mean square (rms) of the stations was only 0.7 mm/year.

164 **Table 5.** IGS stations defined in the site.defaults file of GAMIT to constitute reference frame.

Station ID	City/Country
ANKR	Ankara/Turkey
BUCU	Bucharest/Romania
CRAO	Simeiz/Ukraine
MATE	Metara/Italy
ONSA	Onsala/Switzerland
SOFI	Sofia/Bulgaria
TEHN	Tehran/Iran
TELA	Tel Aviv/Israel
TUBI	Kocaeli/Turkey
WZTR	Koetzting/Germany
ZECK	Zelenchukskaya/Russia

165 Results show that the velocity of the stations inside the Anatolian plate are gathering up to 15-
 166 20 mm/year (Fig 5), which is similar with the previous studies (McClusky et al. 2000, Reilinger et al.
 167 2006, Yavaşoglu et al. 2011).



168 **Figure 5.** GLOBK results for station velocities when Eurasian plate selected as fixed. (A) includes the
 169 Ismetpasa segment, and Destek segment is inside (B). Velocities at the north of the NAF are very
 170 small as expected, where south velocities indicates the Anatolian plate's motion to the west (from
 171 Aladoğan 2017).
 172



173 The GLOBK results for all of the station velocities are used as input for block modelling to
 174 predict the aseismic creep ratio within fault plane in the predefined segments (Table 6, Fig.6).

175 **Table 6.** All cGPS and campaign point velocities and location errors (uncertainties).

Station ID	Velocity(mm/yr)		Error		Station ID	Velocity(mm/yr)		Error	
	V _{EAST}	V _{NORTH}	V _{EAST}	V _{NORTH}		V _{EAST}	V _{NORTH}	V _{EAST}	V _{NORTH}
AKDG	-19.5	5.7	0.1	0.1	KDZU	-14.1	12.3	4.6	4.4
AMAS	-14.5	6.2	0.1	0.1	KKAL	-20.1	1.5	0.1	0.1
ANRK	-22.1	-0.5	0.1	0.1	KRBK	-2.3	0.1	0.1	0.1
BDRG	-7.8	1.1	1.7	1.9	KRBS	-6.4	5.2	1.8	2.1
BILE	-22.8	-4.3	0.1	0.1	KSTM	-1.9	0.6	0.1	0.1
BOLU	-12.8	-0.2	0.1	0.1	KURU	-0.9	0.5	0.1	0.1
BOYT	-2.5	-0.1	0.1	0.1	KVKK	-6.6	0.2	2.1	2.5
BRBY	-10.6	0.6	2.3	2.6	KZDR	-18.7	-4.5	2.1	2.3
BYKY	-6.1	-0.7	1.5	1.8	NAHA	-23.1	-3.2	0.1	0.1
BYYY	-6.8	-1.0	2.1	2.4	ORMN	-0.6	-4.4	1.8	2.0
CANK	-19.4	0.5	0.1	0.1	OZBR	-14.4	1.8	2.2	2.6
CGCS	-19.2	-0.4	3.5	3.7	RDIY	-11.4	5.1	0.1	0.1
CMLD	-21.1	-3.0	0.1	0.1	SAM1	-1.9	1.3	0.2	0.2
CORU	-17.2	3.1	0.1	0.1	SAMN	1.3	-3.0	0.2	0.2
CYLC	-15.5	2.8	2.0	2.4	SIH1	-22.8	-3.6	0.1	0.2
DVBY	-16.6	-2.5	2.0	2.3	SIHI	-22.8	-3.6	0.1	0.2
EREN	-17.6	-2.3	1.9	2.1	SINP	-0.7	0.5	0.1	0.1
ESKS	-23.1	-4.2	0.1	0.1	SIVS	-18.8	7.0	0.1	0.1
FASA	-2.2	1.8	0.1	0.1	SLYE	-8.2	-1.7	2.0	2.3
GIRS	-1.0	2.1	0.1	0.1	SRKY	-10.1	-1.1	2.1	2.5
HCGR	-9.1	3.9	1.7	1.9	SSEH	-12.8	6.1	0.1	0.1
HEND	-6.0	-2.2	0.1	0.1	SUNL	-20.4	2.4	0.1	0.1
HMMP	-14.9	-2.5	2.0	2.0	TOK1	-18.4	6.4	0.1	0.1
HMSL	-13.4	-5.8	1.8	2.1	VEZI	-5.3	2.1	0.1	0.1
HYMN	-20.9	-2.7	0.1	0.1	YYLA	-12.2	-3.3	1.9	2.1
IMLR	-11.5	1.6	2.3	2.6	YZKV	-4.4	1.5	2.6	3.1
IZMT	-5.0	-2.1	0.1	0.1	ZONG	-0.5	-0.7	0.1	0.1

176

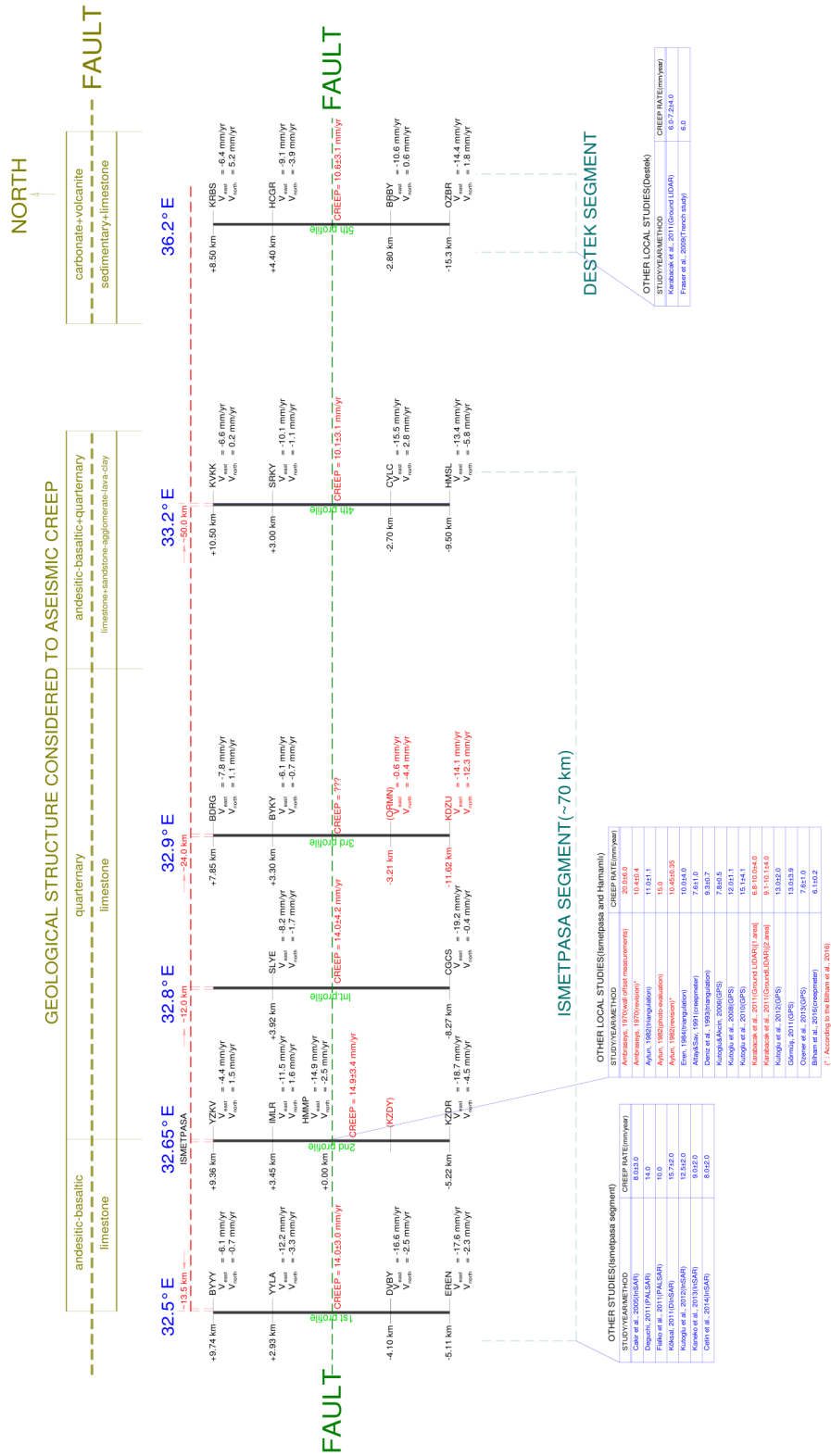


Figure 6. Geological structure related to the aseismic creep, station velocities, estimated creep ratio, and earlier studies around the Ismetpasa and Destek regions (Akbaş et al. 2002., Cetin et al. 2014)



178 Aseismic creep ratio estimated by interpolation through the profiles using surface velocities
179 except the 3rd profile (Table 7). At the Ismetpasa segment, repeatability of the ORMN and KDZU
180 stations indicates abnormal deformation. Therefore, creep estimation for that profile unfeasible.
181 Actually, this is not a drawback for block modelling, because the remaining station velocities are all
182 used to model the region uneventfully.

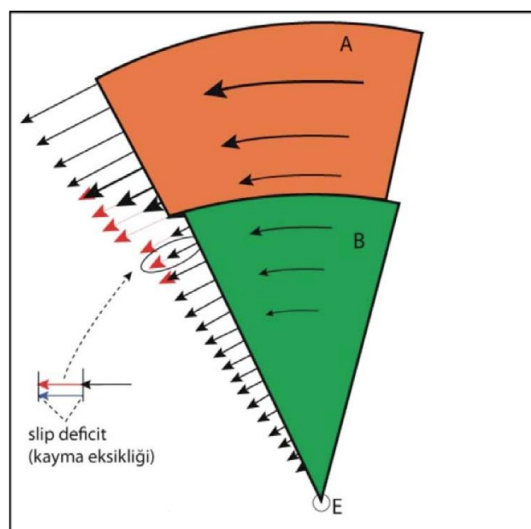
183 **Table 7.** Aseismic creep rate at the Ismetpasa segment.

Profile	Aseismic creep rate(mm/year)
001	14.0±3.0
002	14.9±3.6
005(intermediate)	14.0±4.0
004	10.1±3.0

184 With the calculated surface velocities, Destek segment also have a creep trend through the
185 campaign period. Estimated creep rate in this study according to GLOBK results is 10.6±3.1 mm/year
186 in this region, and indicates aseismic creep similar with the recent studies(Fraser et al. 2009, Karabacak
187 et al. 2011).

188 **Block Modelling**

189 Station velocities are suitable to predict surface and block motions around them locally. On
190 the other hand, observations inside the blocks provide adequate long-term block velocities and
191 rotations with high precision. Blocks generally demonstrate a regular movement, but their motion
192 differ at their boundaries from this overall velocity. They cannot move freely around the faults because
193 of the friction of rocks, generally infer underspeed, may down to none (Fig 7). This difference in the
194 velocity is called "slip deficit", and causes earthquakes after the friction threshold surpasses
195 (Kutoglu&Akcin 2006, McCaffrey 2014, Yavasoglu et al. 2015).

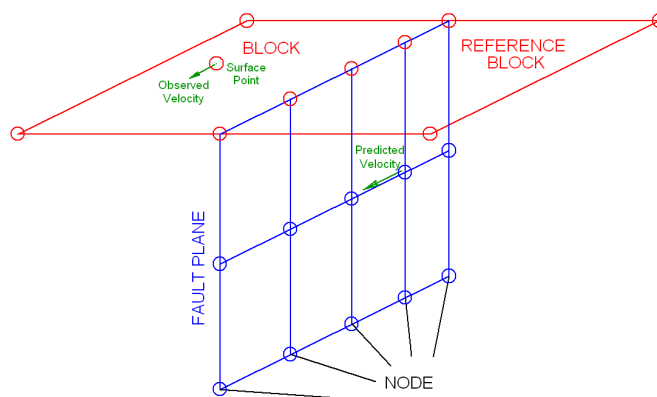


196

197 **Figure 7.** Motions of tectonic blocks around the same Euler pole and slip deficit at their boundaries.
198 Long-term block velocities evolve at the fault zones and gap between them is responsible for strain
199 accumulation and earthquakes (from Cakmak 2010).

200 Slip deficit represents that blocks' expected velocities pass through some deformations
201 regarding the geological structure when approaching the fault zone and frequently decreases. This is
202 based upon the geometry of the fault plane, which can only be predicted and based on the surface
203 velocities. In this context, TDEFNODE software used in this study to predict the fault plane locking
204 interaction regarding the depths, which calculates variations of the block motions, strain accumulation
205 within the blocks, and rotations through interseismic or coseismic period (Okada 1985, McCaffrey
206 2009, Yavaşoğlu 2011).

207 Basic input for the software includes GPS velocities, blocks with Euler poles, user's fault
208 geometry prediction and locking depth, generally acquired after seismic researches. Interacting blocks
209 represented as elastic blocks and assumed to have elastic deformation because of their rotation
210 around Euler poles. All of the defined system assumed to float inside a half-space where one of the
211 blocks is fixed and have zero strain or movement. Fault geometry defined by the user with nodes, and
212 their locking ratios (ϕ) can be defined manually or as a function of depth (Fig. 8). Then, the software
213 predicts the underground velocities based on the routines of Okada (1985), and estimates the surface
214 velocities according the defined values. Fault geometry estimation is the key feature to minimize the
215 difference between observed and predicted surface velocities with the help of χ^2 test result, which
216 represents the accuracy of the entire model (McCaffrey 2002, Aktuğ ve Çelik 2008, Yavasoglu et al.
217 2011).

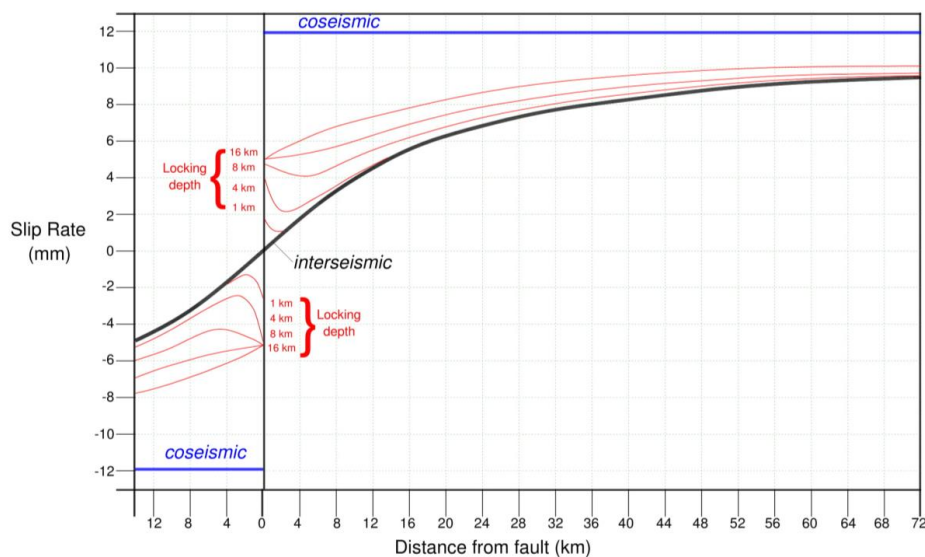


218

219 **Figure 8.** Fault plane geometry defined to the control file of TDEFNODE. Nodes divides the fault plane
220 into sub-regions to defined depths and their locking ratio may differ from each other.

221 TDEFNODE can be used for interacting blocks for interseismic strain accumulation, but also for
222 faults which are partially or fully free slipping, like aseismic creep. Software's model is suitable to define
223 the locking ratios of all nodes independently from (0-1). (0) represents that the fault at that node is
224 freely slipping, and (1) for a fully locked node. This allows user to define the fault plane with layers by
225 using depth contours, and to predict the fault plane if these layers are partially or fully locked (Url-2).

226 Aseismic creep is an earthquake-free motion along the earth surface, but in some cases it's
227 hard to detect whether this motion is a free slipping event or and an interseismic movement. Thus, the
228 observation network around the fault plane should be planned carefully regarding the ± 3 -10 km station
229 locations mentioned before (Fig 9).



230

231 **Figure 9.** Slip rate along a fault plane during interseismic and coseismic events. Blue lines represents
232 the coseismic, and black line represents the interseismic behaviour, where red lines demonstrates
233 the aseismic creep ratios at two sides of the fault for different locking depths (after Yavasoglu et al.
234 2015).

235 *Figure 9* demonstrates the suitable distances to detect aseismic creep. If an aseismic creep
236 suspected on a fault plane, then the optimum locations for the observation stations should be around
237 3 and 10 km on both sides of the fault, and can be resolved from the interseismic movements.
238 Therefore, observation stations, mentioned before, established around the fault as profiles to detect
239 this discrepancies, and to detect the main locking depth of the fault and attenuation depths for the
240 creep event. Their locations are suitable to evaluate both creeping ratios and locking depths of the
241 faults.

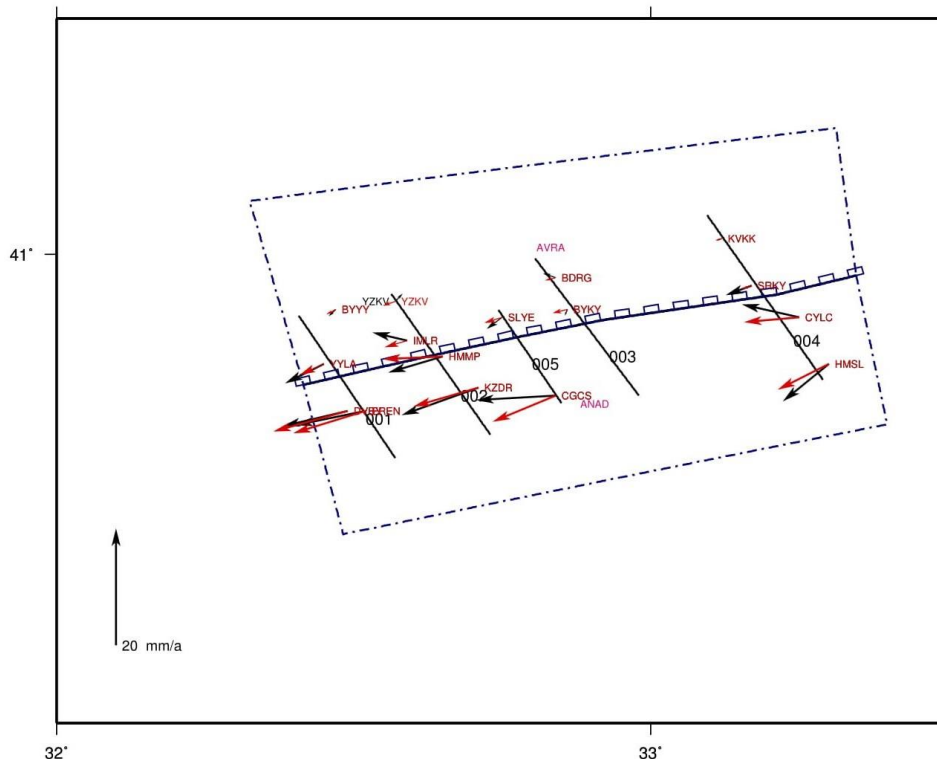
242 Discussion

243 Station velocities all around the region indicates the relative motion of the Anatolian plate
244 regarding the Eurasian plate. Movements ranges between 15-24 mm/year inside the southern plate
245 where the northern motion reaches down to ~1 mm/year. This result is consistent with the previous
246 studies (~24±2 mm/year)(McClusky et al. 2000, Reilinger et al. 2006, Yavasoglu et al. 2011). In addition,
247 model locking depths and results are similar with a more recent study with InSAR, which indicates the
248 locking depth of the fault at Ismetpasa segment around 13-17 km and long-term tectonic movement
249 about 24-30 mm/year (Hussain et al. 2018).



250 Inspected segments' special features revealed by the network established near the fault plane.
251 Regarding the surface velocities of the observation points, profiles on both Ismetpasa and Destek
252 segments indicates movements. This ranges between 10.1-14.9 mm/year and 10.6 mm/year for
253 Ismetpasa and Destek segments, respectively.

254 On the other side, modeled fault plane evaluation for observed and calculated station
255 movements demonstrates similar results with the locking depths of the both creeping and seismogenic
256 layers (Fig. 10). Station velocities on the south of the NAF faster than the north-end as expected (Fig.
257 11). Regarding the long-term geodetic block motions, modeled weighted locking ratios indicates a
258 13.0 ± 3.3 mm/year of aseismic creep all over the Ismetpasa segment. This movement does not include
259 the whole fault plane, thus the creeping layer seems to slip freely to 4.5 km depths from the surface
260 and decays between 4.5-6.75 km. The seismic data and previous studies (Cakir et al. 2005, Yavaşoğlu
261 et al. 2011, Hussain et al. 2019) indicates the locking depth all over the fault as ~ 15 km. This result
262 demonstrates the fully locked portion of the fault plane is between 6.75-15 km, which supported by
263 the χ^2 test result.



264
265 **Figure 10.** Model area for Ismetpasa segment with Eurasian plate (AVRA) on the north and Anatolian
266 plate (ANAD) on the south (dashed lines), divided by the creeping segment of the NAF. Black and red
267 arrows represent the observed and modeled velocities respectively, obtained from GAMIT/GLOBK



268 and TDEFNODE. Five profiles are numbered from west to east with 001 to 004, where 005 represents
 269 the intermediate profile established during the 1st campaign. Two stations (SLYE and CGCS) on the
 270 south-end of the profile 003 removed from the model due to unexpected velocities.

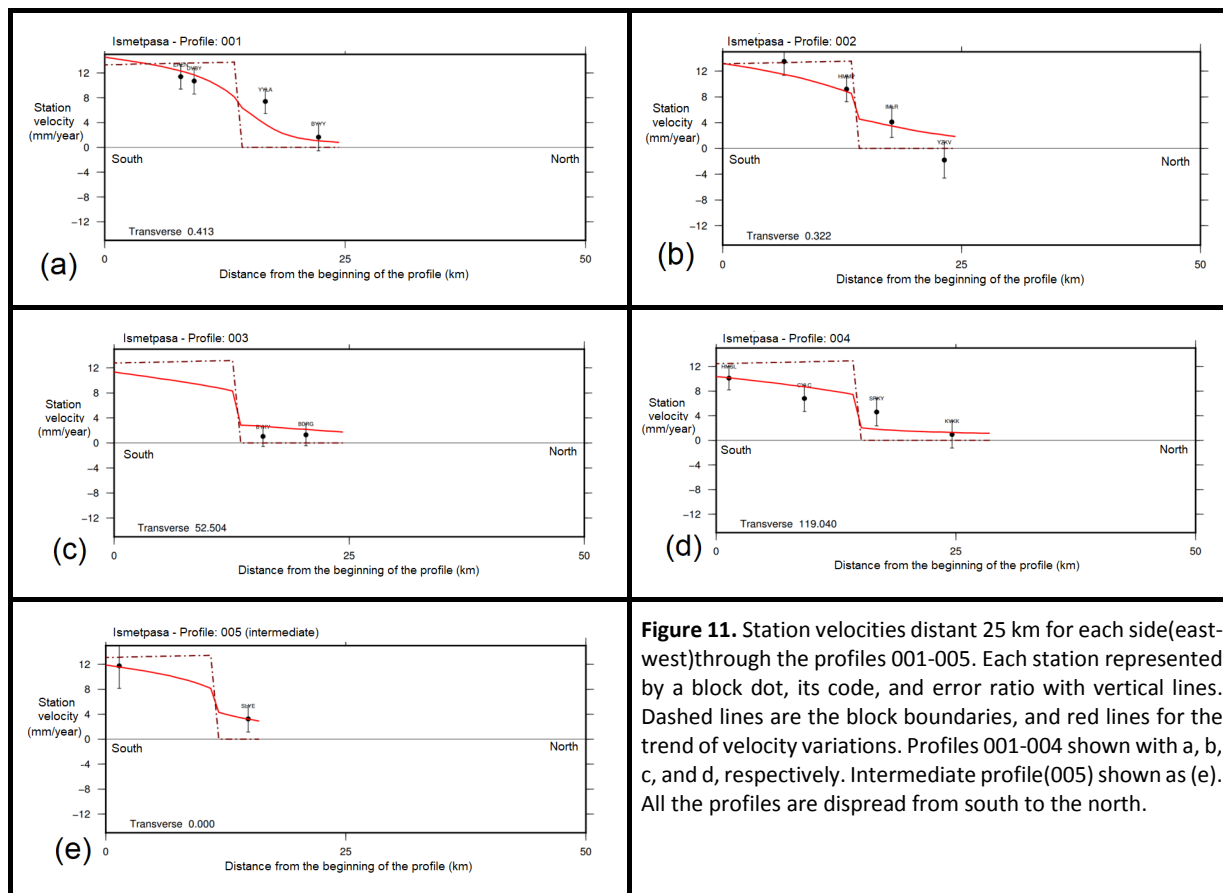
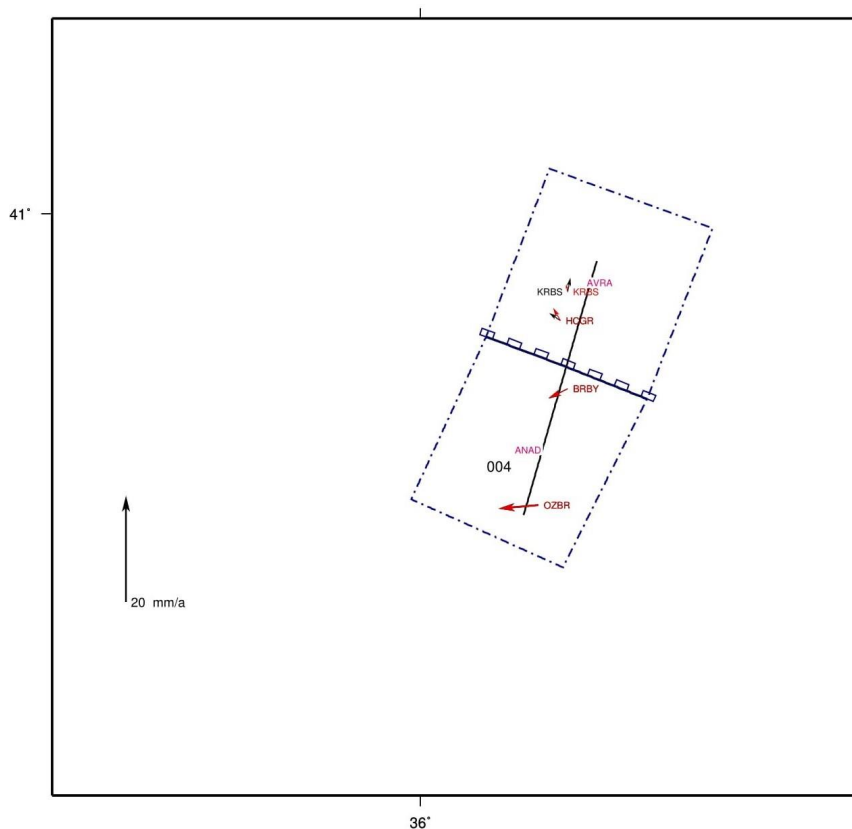


Figure 11. Station velocities distant 25 km for each side (east-west) through the profiles 001-005. Each station represented by a block dot, its code, and error ratio with vertical lines. Dashed lines are the block boundaries, and red lines for the trend of velocity variations. Profiles 001-004 shown with a, b, c, and d, respectively. Intermediate profile (005) shown as (e). All the profiles are dispread from south to the north.

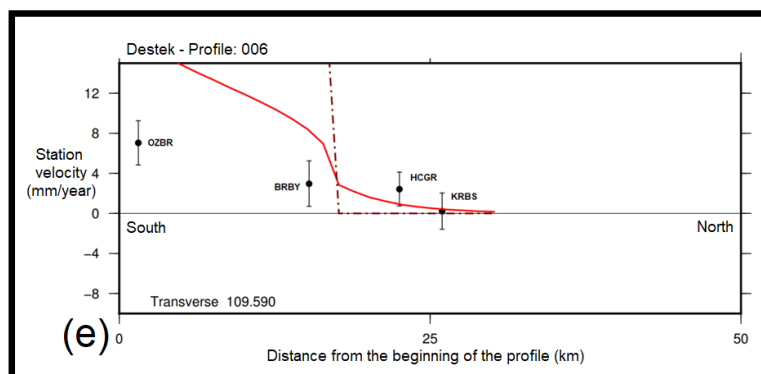
271

272 Destek segment also have similar results for the observed and modeled velocities (Fig 12). The
 273 surface velocities for the profile (006) at this region indicates velocity differences (Fig 13). On the other
 274 hand, modeled fault plane indicates the creeping segment to 4.3 km depths and decays linearly
 275 between 4.3-6.0 km. The remaining layer of the part seems to be fully locked down to the seismogenic
 276 layer. Free slipping portion have a 9.6 mm/year which is similar with the estimated surface velocities
 277 (10.6 ± 3.1 mm/year). The χ^2 test result and the seismic data confirms the accuracy of the model.



278
 279
 280
 281
 282

Figure 12. Model area for Destek segment with Eurasian plate(AVRA) on the north and Anatolian plate(ANAD) on the south(dashed lines), divided by the creeping segment of the NAF. Black and red arrows represent the observed and modeled velocities respectively, obtained from GAMIT/GLOBK and TDEFNODE. 004 represents the profile in the area.



283
 284
 285
 286

Figure 13. Station velocities and profile (006) for the Destek profile. Each station represented by a black dot, its code, and error ratio with vertical lines. Dashed lines are the block boundaries, and red lines for the trend of velocity variations. Profile dispread from south to the north.



287 On the other hand, Paleomagnetic data indicates a predominantly clockwise rotation of the
288 blocks bordered by the faults between Ismetpaşa and Destek segments. Examining the results with
289 this study promotes this behaviour with the GPS field of the region, especially on the Anatolian side of
290 the NAF (Figure 10&12) (İşseven & Tüysüz, 2006).

291 We find no clear evidence for attenuation at both segments, on the contrary, a slight increase
292 at Ismetpasa and almost 50% of an increase at Destek regarding the previous studies. The frequency
293 of this phenomenon at both sites is unclear, but results at *Hussain et al. (2018)* assists this argument,
294 that the creep event will continue until the next large-scale earthquake.

295 Conclusion

296 NAF reported to have a creeping phenomena at Ismetpasa since 1970 and observed with
297 different techniques for a long time period with a recent discovery at Destek. All the previous studies
298 concentrate on the whole segments or at least some regions along these segments. With this study, a
299 GPS network covering the whole Anatolian region along the NAF established for the first time and
300 results for the velocity area used as input for block modeling. Also, the first GPS network covering
301 Destek segment established during this study.

302 Network design and location of the observation points distinguished according to the main
303 locking depth of the NAF and attenuation depth for the aseismic creep event. Model results show
304 similar outcomes for both Ismetpasa and Destek segments, where locking depth for these segments
305 are ~15 km, and attenuation for the creeping layer depths varies between ~4-6 km.

306 Through all the models, results for this study indicates that the creeping behaviour still
307 continues at both Ismetpasa and Destek segments, with a ratio of 13.0 ± 3.3 mm/year and 10.6 ± 3.1
308 mm/year, respectively. Block modeling and seismic data indicates that the creeping segment does not
309 reach to the bottom of the seismogenic layer (~15 km) and limited to some depths, which may not
310 prevent a medium-large scale earthquake in the long term. In addition, we found no evidence for the
311 attenuation of aseismic creep. Also, the frequency of this movement at Ismetpasa is unclear and it is
312 not possible to predict the aseismic creep ratio precisely for long-term, but results might indicate a
313 small increase in the trend regarding the previous studies in the region.

314 On the other hand, the creeping ratio seems to increase almost 50% at the Destek segment
315 considering the previous studies, which might indicate a relief at that segment. However, according to
316 the model, aseismic creep is limited to some depths (~6.0 km) and creep ratio is smaller than the long
317 term block movements. The increasing trend is not sufficient to release all the strain in this segment.
318 This might indicate strain accumulation on the both ends of the segment.



319 The established network by this study should be monitored periodically for the assessment of
320 the frequency of aseismic creep precisely, which may include possible clues for a clear fault plane
321 definition and earthquakes. In addition, results indicates that this creep event will be monitored to the
322 next earthquake, which might reveal valuable information for fault zone layout model.

323 Acknowledgements

324 This paper is based on the PhD thesis of Mehmet Nurullah Alkan with the title of “Kuzey
325 Anadolu Fayı (KAF) Bolu-Çankırı ve Amasya Bölgelerindeki Asismik Tektonik Yapının Periyodik GPS
326 Ölçümleri ile Belirlenmesi”, and supported by the Coordinatorship of Scientific Research Projects (BAP)
327 of Hitit University (project no: MYO19001.14.001), Istanbul Technical University (project no:
328 15.FEN.BİL.16), and Afyon Kocatepe University (project no: 38146). We also would like to thank to all
329 participant in this project who helped during the field and software processes. In addition, we
330 appreciate the great equipment and software support of Afyon Kocatepe University and Ibrahim
331 Tiryakioglu. The maps in this paper created by using the GMT scripts provided by TDEFNODE software
332 (McCaffrey 2002, URL-2).

333 REFERENCES

- 334 Akbaş, B., Akdeniz, N., Aksay, A., Altun, İ., Balcı, V., Bilginer, E., Bilgiç, T., Duru, M., Ercan, T., Gedik, İ.,
335 Günay, Y., Güven, İ.H., Hakyemez, H.Y., Konak, N., Papak, İ., Pehlivan, Ş., Sevin, M.,
336 Şenel, M., Tarhan, N., Turhan, N., Türkecan, A., Ulu, Ü., Uğuz, M.F., Yurtsever, A. ve
337 diğerleri: Türkiye Jeoloji Haritası Maden Tetkik ve Arama Genel Müdürlüğü Yayını.
338 Ankara, Türkiye, 2002.
- 339 Aktuğ, B., Çelik, R.N.: Jeodezik ölçüler ile deprem kaynak parametrelerinin belirlenmesi, İTÜ dergisi, 7,
340 89-102, 2008.
- 341 Aladoğan. K., Tiryakioglu, İ., Yavaşoğlu, H., Alkan, R.M., Alkan, M.N., Köse, Z., İlçi, V., Ozulu, İ.M.,
342 Tomuş, F.E., Şahin, M.: Kuzey Anadolu Fayı Bolu-Çorum Segmenti Boyunca Yer
343 Kabuğu Hareketlerinin GNSS Yöntemiyle İzlenmesi, Afyon Kocatepe Üniversitesi Fen ve
344 Mühendislik Bilimleri Dergisi, 17(3), 997-1003, doi: 10.5578/fmbd.60762, 2017.
- 345 Altay, C., Sav, H: Continuous creep measurement along the North Anatolian fault zone, Bulletin of
346 Geological Congress of Turkey, 6, 77-84, 1991.
- 347 Ambraseys, N.N.: Some characteristic features of the Anatolian fault zone, Tectonophysics, 9, 143-165,
348 [https://doi.org/10.1016/0040-1951\(70\)90014-4](https://doi.org/10.1016/0040-1951(70)90014-4), 1970.
- 349 Aytun, A.: Creep measurements in the İsmetpaşa region of the North Anatolian Fault Zone,
350 Multidisciplinary Approach to Earthquake Prediction, 2, 279-292,
351 https://doi.org/10.1007/978-3-663-14015-3_20, 1982.



- 352 Bilham, R., Ozener, H., Mencin, D., Dogru, A., Ergintav, S., Cakir, Z., Aytun, A., Aktug, B., Yilmaz, O.,
353 Johnson, W., Mattioli, G.: Surface creep on the North Anatolian Fault at Ismetpasa,
354 Turkey, 1944-2016, *Journal of Geophysical Research: Solid Earth*, 121, 7409-7431,
355 <https://doi.org/10.1002/2016JB013394>, 2016.
- 356 Bohnhoff, M., Martinez-Garzon, P., Bulut, F., Stierle, E., Ben-Zion, Y.: Maximum earthquake magnitudes
357 along different sections of the North Anatolian fault zone, *Technophysics*, 674, 147-
358 165, <http://doi.org/10.1016/j.tecto.2016.02.028>, 2016.
- 359 Cakir, Z., Akoglu, A.M., Belabbes, S., Ergintav, S., Meghraoui, M.: Creeping along the Ismetpasa section
360 of the North Anatolian fault(Western Turkey): Rate and extent from InSAR, *Earth and
361 Planetary Science Letters*, 238, 225-234, doi: 10.1016/j.epsl.2005.06.044, 2005.
- 362 Cakir, Z., Ergintav, S., Özener, H., Doğan, U., Akoglu, A.M., Meghraoui, M., Reilinger, R.: Onset of
363 aseismic creep on major strike-slip faults, *Geology*, 40/12, 1115-1118, doi:
364 10.1130/G33522.1, 2012.
- 365 Cakmak, R.: Jeodezik çalışmalarla Marmara Bölgesinde deprem döngüsünün belirlenmesi ve
366 modellerle açıklanması, Ph.D. thesis, İstanbul Teknik Üniversitesi Fen Bilimleri
367 Enstitüsü, Turkey, 131 pp., 2010.
- 368 Cetin, E., Cakir, Z., Meghraoui, M., Ergintav, S., Akoglu, A.M.: Extent and distribution of aseismic slip on
369 the Ismetpaşa segment of the North Anatolian Fault(Turkey) from Persistent Scatterer
370 InSAR, *Geochemistry, Geophysics, Geosystems*, 15, 2883-2894,
371 <https://doi.org/10.1002/2014GC005307>, 2014.
- 372 Deguchi, T.: Detection of fault creep around NAF by InSAR time series analysis using PALSAR data,
373 *Proceedings of SPIE*, 8179, doi: 10.1117/12.898478, 2011.
- 374 Deniz, R., Aksoy, A., Yalin, D., Seeger, H., Hirsch, O.: Determination of crustal movement in Turkey by
375 terrestrial geodetic methods, *Journal of Geodynamics*, 18, 13-22,
376 [https://doi.org/10.1016/0264-3707\(93\)90024-Z](https://doi.org/10.1016/0264-3707(93)90024-Z), 1993.
- 377 Emre, Ö., Duman, T.Y., Özalp, S., Şaroğlu, F., Olgun, Ş., Elmacı, H., Çan, T.: Active fault database of
378 Turkey, *Bull. Earthquake Eng.*, 16, 3229-3275, 2018.
- 379 Eren, K.: (1984). Strain analysis along the North Anatolian fault by using geodetic surveys,
380 *Bull.Geodesique*, 58(2), 137-149, 1984.
- 381 Fialko, Y., Kaneko, Y., Tong, X., Sandwell, D.T., Furuya, M.: Investigation of interseismic deformation
382 along the central section of the North Anatolian fault(Turkey) using InSAR observations
383 and earthquake-cycle simulations, *American Geophysical Union, Fall Meeting abstract
384 #T31E-08*, 2011.
- 385 Fraser, J., Pigati, J.S., Hubert-Ferrari, A., Vanneste, K., Avsar, U., Altinok, S.: A 3000-Year Record of
386 Ground-Rupturing Earthquakes along the North Anatolian Fault near Lake Ladik,
387 Turkey, *Bulletin of the Seismological Society of America*, 99, 2651-2703, doi:
388 10.1785/0120080024, 2009.
- 389 Görmüş, K.S.: Kuzey Anadolu Fayı İsmetpaşa segmentindeki krip hızı değişiminin izlenmesi, Ph.D. thesis,
390 Zonguldak Karaelmas Üniversitesi Fen Bilimleri Enstitüsü, Turkey, 97 pp., 2011.
- 391 Halıcıoğlu, K., Özener, H., Ünlütepe, A.: Fay parametreleri ve kontrol ağlarının tasarımı, 12.Türkiye
392 Harita Bilimsel ve Teknik Kurultayı, Ankara, 11-15 May 2009, 2009.



- 393 Herring, T., King, R.W., Floyd, M.A., McClusky, S.C.: Global Kalman filter VLBI and GPS analysis program,
394 Department of Earth Atmospheric, And Planetary Sciences, Massachusetts Institute of
395 Technology, 2015a.
- 396 Herring, T., King, R.W., Floyd, M.A., McClusky, S.C.: Introduction to GAMIT/GLOBK, Department of
397 Earth, Atmospheric, And Planetary Sciences, Massachusetts Institute of Technology,
398 2015b.
- 399 Hussain, E., Wright, T.J., Walters, R.J., Bekaert, D.P.S., Lloyd, R., Hooper, A. Constant strain
400 accumulation rate between major earthquakes on the North Anatolian Fault, Nature
401 Communications, 9, 1392, doi: 10.1038/s41467-018-03739-2, 2018.
- 402 İşseven, T., Tüysüz, O.: Paleomagnetically defined rotations of fault-bounded continental block in the
403 North Anatolian Shear Zone, North Central Anatolia. Journal of Asian Earth Sciences,
404 28, 469-479, doi:10.1016/j.jseaeas.2005.11.012, 2006.
- 405 Karabacak, V., Altunel, E., Cakir, Z.: Monitoring aseismic surface creep along the North Anatolian
406 Fault(Turkey) using ground-based LIDAR, Earth and Planetary Science Letters, 304, 64-
407 70, doi:10.1016/j.epsl.2011.01.017, 2011.
- 408 Kaneko, Y., Fialko, Y., Sandwell, D.T., Tong, X., Furuya, M.: Interseismic deformation and creep along
409 the central section of the North Anatolian Fault(Turkey): InSAR observations and
410 implications for rate-and-state friction properties, Journal of Geophysical Research:
411 Solid Earth, 118, 316-331, doi: 10.1029/2012jb009661, 2013.
- 412 Ketin, İ.: Kuzey Anadolu Fayı hakkında, Maden Tetkik ve Arama Dergisi, 1969.
- 413 Ketin, İ.: San Andreas ve Kuzey Anadolu Fayları arasında bir karşılaştırma, Türkiye Jeoloji Kurumu
414 Bülteni, 19, 149-154, 1976.
- 415 Köksal, E. Yüze deformasyonlarının Diferansiyel InSAR Tekniği ile Belirlenmesi: İsmetpaşa Örneği.
416 Ph.D. thesis, Zonguldak Karaelmas Üniversitesi Fen Bilimleri Enstitüsü, Turkey, 136 pp.,
417 2011.
- 418 Kutoglu, H.S., Akcin, H.: Determination of the 30-year creep trend on the İsmetpaşa segment of the
419 North Anatolian Fault using an old geodetic network, Earth Planets Space, 58, 937-
420 942, https://doi.org/10.1186/BF03352598, 2006.
- 421 Kutoglu, H.S., Akcin, H., Kemaldere, H., Gormus, K.S.: Triggered creep rate on İsmetpasa segment of
422 the North Anatolian Fault, Natural Hazards and Earth System Sciences, 8, 1369-1373,
423 https://doi.org/10.5194/nhess-8-1369-2008, 2008.
- 424 Kutoğlu, H.Ş., Akçin, H., Görmüş, K.S., Kemaldere, H.: Kuzey Anadolu Fayı İsmetpaşa segmentinde
425 gerçekleştirilen jeodezik çalışmalar, 12.Türkiye Harita ve Bilimsel Kurultayı, Ankara, 11-
426 15 May 2009, 2009.
- 427 Kutoglu, H.S., Akcin, H., Gundogdu, O., Gormus, K.S., Koksal, E.: Relaxation on the İsmetpasa segment
428 of the North Anatolian Fault after the Golcuk $M_w=7.4$ and Duzce $M_w=7.2$ shocks, Nat.
429 Hazards Earth Syst.Sci., 10, 2653-2657, DOI: 10.5194/nhess-10-2653-2010, 2010.
- 430 Kutoglu, H.S., Gormus, K.S., Deguchi, T., Koksal, E., Kemaldere, H., Gundogdu, O.: Can a creeping
431 segment become a monitor before destructive major earthquakes, Natural Hazards,
432 65, 2161-2173, DOI: 10.1007/s11069-012-0466-0, 2013.
- 433 McCaffrey, R.: Crustal block rotations and plate coupling, Plate Boundary Zones, Geodynamic Series,
434 30, 101-122, https://doi.org/10.1029/GD030p0101, 2002.



- 435 McCaffrey, R.: Time-dependent inversion of three-component continuous GPS for steady and transient
436 sources in northern Cascadia, *Geophysical Research Letters*, 36-7, L07304, doi:
437 10.1029/2008GL036784, 2009.
- 438 McCaffrey, R.: Interseismic locking on the Hikurangi subduction zone: Uncertainties from slow-slip
439 events, *Journal of Geophysical Research: Solid Earth*, 119: 7874-7888,
440 <https://doi.org/10.1002/2014JB010945>, 2014.
- 441 McClusky, S., Balassanian, S., Barka, A., Demir, C., Ergintav, S., Georgiev, I., Gurkan, O., Hamburger, M.,
442 Hurst, K., Kahle, H., Kastens, K., Kekelidze, G., King, R., Kotzev, V., Lenk, O., Mahmoud,
443 S., Mishin, A., Nadriya, M., Ouzounis, A., Paradissis, D., Peter, Y., Prilepin, M., Reilinger,
444 R., Sanli, I., Seeger, H., Tealeb, A., Toksoz, M.N., Veis, G.: Global Positioning System
445 constraints on plate kinematics and dynamics in the eastern Mediterranean, *Journal*
446 *of Geophysical Research*, 105, 5695–5719, DOI: 10.1029/1996JB900351, 2000.
- 447 Okada, Y.: Internal deformation due to shear and tensile faults in a half-space. *Bull.Seismol.Soc.Am.*,
448 75: 1135-1154, 1985.
- 449 Ozener, H., Dogru, A., Turgut, B.: Quantifying aseismic creep on the Ismetpasa segment of the North
450 Anatolian Fault Zone(Turkey) by 6 years of GPS observations, *Journal of Geodynamics*,
451 67, 72-77, DOI: 10.1016/j.jog.2012.08.002, 2013.
- 452 Poyraz, F., Tatar, O., Hastaoğlu, K.Ö., Türk, T., Gürsoy, T., Gürsoy, Ö., Ayazlı, İE.: Elastik atım teorisi:
453 Kuzey Anadolu Fay Zonu örneği, 13.Türkiye Harita Bilimsel ve Teknik Kurultayı, Ankara,
454 18-22 April 2011, 2011.
- 455 Reid, H.F.: The Mechanics of the Earthquake, The California Earthquake of April 18, 1906. Report of the
456 State Investigation Commission, Carnegie Institution of Washington, 2: 16-28, 1910.
- 457 Reilinger, R., McClusky, S., Vernant, P., Lawrance, S., Ergintav, S., Cakmak, R., Ozener, H., Kadirov, F.,
458 Guliev, I., Stepanyan, R., Nadariya, M., Habubia, G., Mahmoud, S., Sakr, K., ArRajehi,
459 A., Paradissis, D., Al-Aydrus, A., Prilepin, M., Guseva, T., Evren, E., Dmitrova, A., Filikov,
460 S.V., Gomez, F., Al-Ghazzi, R., Karam, G.: GPS constraints on continental deformation
461 in the Africa-Arabia, Eurasia continental collision zone and implications for the
462 dynamics of plate interactions, *Journal of Geophys.Research-Solid Earth*, 111, 1-
463 26(B05411), <https://doi.org/10.1029/2005JB004051>, 2006.
- 464 Rousset, B., Jolivet, R., Simons, M., Lasserre, C., Riel, B., Milillo, P., Çakir, Z., Renard, F.: An aseismic slip
465 transient on the North Anatolian Fault, *Geophysical Research Letters*, 43, 3254-3262,
466 <http://dx.doi.org/10.1002/2016GL068250>, 2016.
- 467 Schmidt, D.A., Bürgmann, R., Nadeau, R.M., d'Alessio, M.: Distribution of aseismic slip rate on the
468 Hayward fault inferred from seismic and geodetic data, *Journal of Geophysical*
469 *Research*, 110, B08406, <https://doi.org/10.1029/2004JB003397>, 2005.
- 470 Şengör, A.M.C., Tüysüz, O., İmren, C., Sakıncı, M., Eyidoğan, H., Görür, N., Pichon, X.L., Rangin, C.: The
471 North Anatolian Fault: A new look, *Annu.Rev.Earth Planet*, 33, 37-112,
472 <https://doi.org/10.1146/annurev.earth.32.101802.120415>, 2005.
- 473 Şaroğlu, F., Barka, A.: Deprem sonrası devam eden uzun dönem yerdeğiştirmelerin anlamı ve önemi,
474 *Jeofizik*, 9, 339-343, 1995.
- 475 Taskin, G., Uskuplu, S., Saygin, H., Ergintav, S.: Optimization of GPS observation strategy for
476 improvement of tectonic measurements. The IASTED International Conference on
477 Applied Simulation and Modelling, Spain, 03-05 September 2003, 2003.



- 478 Wei, M., Sandwell, D., Fialko, Y., Bilham, R.: Slip on faults in the Imperial Valley triggered by the 4 April
479 2010 Mw 7.2 El Mayor-Cucapah earthquake revealed by InSAR, *Geophysical Research*
480 *Letters*, 38, L01308, doi: 10.1029/2010gl045235, 2011.
- 481 Yavasoglu, H., Alkan, M.N., Ozulu, I.M., Ilci, V., Tombus, F.E., Aladogan, K., Sahin, M., Tiryakioglu, I.,
482 Kivrak, S.O.: Recent tectonic features of the central part(Bolu-Corum) of the North
483 Anatolian Fault, *Hittite Journal of Science and Engineering*, 2/1, 77-83, doi:
484 10.17350/HJSE19030000011, 2015.
- 485 Yavaşoğlu, H., Tari, E., Tüysüz, O., Çakır, Z., Ergintav, S.: Determining and modeling tectonic movements
486 along the central part of the North Anatolian Fault(Turkey) using geodetic
487 measurements, *Journal of Geodynamics*, 51, 339-343,
488 <https://doi.org/10.1016/j.jog.2010.07.003>, 2011.
- 489 <http://funnel.sfsu.edu/creep/WhatsCreepPage.html>, last access: 19.12.2018.
- 490 <http://www.web.pdx.edu/~mccaf/defnode.html>, last access: 20.12.2018.